

1 **Soil moisture control on sap-flow response to biophysical factors in a desert-shrub**
2 **species, *Artemisia ordosica***

3 **Authors:** Tianshan Zha^{1,3*#}, Duo Qian^{2#}, Xin Jia^{1,3}, Yujie Bai¹, Yun Tian¹, Charles P.-A.
4 Bourque⁴, Wei Feng¹, Bin Wu¹, Heli Peltola⁵

5 ^{1.} Yanchi Research Station, School of Soil and Water Conservation, Beijing Forestry
6 University, Beijing 100083, China

7 ^{2.} Beijing Vocational College of Agriculture, Beijing 102442, China

8 ^{3.} Key Laboratory of State Forestry Administration on Soil and Water Conservation,
9 Beijing Forestry University, Beijing, China

10 ^{4.} Faculty of Forestry and Environmental Management, 28 Dineen Drive, PO Box 4400,
11 University of New Brunswick, New Brunswick, E3B5A3, Canada

12 ^{5.} Faculty of Science and Forestry, School of Forest Sciences, University of Eastern
13 Finland, Joensuu, FI-80101, Finland

14 #These authors contributed equally to this work.

15

16

17 **Short title: Sap flow in *Artemisia ordosica***

18

19

20 *Correspondence to:* T. Zha (tianshanzha@bjfu.edu.cn),

21

22 **Author Contribution Statement:**

23 Dr.'s Duo Qian and Tianshan Zha contributed equally to the design and implementation of
24 the field experiment, data collection and analysis, and writing the first draft of the manuscript.

25 Dr. Xin Jia gave helpful suggestions concerning the analysis of the field data and contributed
26 to the scientific revision and editing of the manuscript.

27 Prof. Bin Wu contributed to the design of the experiment.

28 Dr.'s Charles P.-A. Bourque and Heli Peltola contributed to the scientific revision and editing
29 of the manuscript.

30 Yujie Bai, Wei Feng, and Yun Tian were involved in the implementation of the experiment
31 and in the revision of the manuscript.

32

33 **Key Message:** This study provides a significant contribution to the understanding of
34 acclimation processes in desert-shrub species to drought-associated stress in dryland
35 ecosystems

36

37 **Conflict of Interest:**

38 This research was financially supported by grants from the National Natural Science
39 Foundation of China (NSFC No. 31670710, No. 31670708), the National Basic Research
40 Program of China (Grant No. 2013CB429901), and by the Academy of Finland (Project No.
41 14921). The project is related to the Finnish-Chinese collaborative research project,
42 EXTREME (2013-2016), between Beijing Forestry University and the University of Eastern
43 Finland, and USCCC. We appreciate Dr. Ben Wang, Sijing Li, Qiang Yang, and others for
44 their help with the fieldwork. **The authors declare that they have no conflict of interest.**

45

46 **Abstract:** Current understanding of acclimation processes in desert-shrub species to drought
47 stress in dryland ecosystems is still incomplete. In this study, we measured sap flow in
48 *Artemisia ordosica* and associated environmental variables throughout the growing seasons
49 of 2013-2014 (May-September period of each year) to better understand the environmental
50 controls on the temporal dynamics of sap flow. We found that the occurrence of drought in
51 the dry year of 2013 during the leaf-expansion and leaf-expanded periods caused sap flow
52 per leaf area (J_s) to decline significantly, resulting in transpiration being 34% lower in 2013
53 than in 2014. Sap flow per leaf area correlated positively with radiation (R_s), air temperature
54 (T), and vapor pressure deficit (VPD), when volumetric soil water content (VWC) was > 0.10
55 $\text{m}^3 \text{m}^{-3}$. Diurnal J_s was generally ahead of R_s by as much as 6 hours. This lag time, however,
56 decreased with increasing VWC. Relative response of J_s to the environmental variables (i.e.,
57 R_s , T , and VPD) varied with VWC, J_s being more biologically-controlled with a low
58 decoupling coefficient and low sensitivity to the environmental variables during periods of
59 dryness. According to this study, soil moisture is shown to control sap-flow (and, therefore,
60 plant-transpiration) response in *Artemisia ordosica* to diurnal variations in biophysical
61 factors. The findings of this study add to the knowledge of acclimation processes in desert-
62 shrub species under drought-associated stress. This knowledge is essential to model desert-
63 shrub-ecosystem functioning under changing climatic conditions.

64 **Keywords:** sap flow; transpiration; cold-desert shrubs; environmental stress; volumetric soil
65 water content

66

67

68 **1. Introduction**

69 Due to the low amount of precipitation and high potential evapotranspiration in desert
70 ecosystems, low soil water availability limits both plant water- and gas-exchange and, as a
71 consequence, limits vegetation productivity (Razzaghi et al., 2011). Therefore, it is important
72 to understand the mechanisms controlling the vegetation-water dynamics under rapidly
73 changing environments (Jacobsen et al., 2007). Grass species are gradually being replaced
74 by shrub and semi-shrub species in arid and semi-arid areas of northwestern China (Yu et al.,
75 2004). This progression is predicted to continue under a changing climate (Asner et al.,
76 2003;Houghton et al., 1999; Pacala et al., 2001). This is mostly because desert shrubs are
77 able to adapt to hot-dry environments by modifying their morphological characteristics, e.g.,
78 by (1) minimizing plant-surface area directly exposed to sun and hot air, (2) producing thick
79 epidermal hairs, (3) thickening cuticle, (4) recessing stomata into leaves (Yang and Zhu,
80 2011), and (5) increasing root-to-shoot ratios (Eberbach and Burrows, 2006; Forner et al.,
81 2014). Also, acclimation of physiological characteristics of plants under water stress, by way
82 of e.g., water potential, osmotic regulation, anti-oxidation, and photosynthetic characteristics,
83 assist the plants to maintain a hydrological balance (Huang et al., 2011a). Changes in stomatal
84 conductance and, thus, transpiration may equally affect plant water use efficiency (Pacala et
85 al., 2001; Vilagrosa et al., 2003).

86 Sap flow can accurately reflect water consumption during plant transpiration. It
87 maintains ecosystem balance through the soil-plant-atmosphere continuum, but is often
88 affected by environment factors (Huang *et al.*, 2010; Zhao et al., 2016). In recent studies, sap
89 flow in *Tamarix elongate* has been observed to be controlled by solar radiation and air

90 temperature, whereas in *Caragana korshinskii* vapor pressure deficit and solar radiation
91 appear to be more important (Jacobsen et al., 2007; Xia et al., 2008). In *Elaeagnus*
92 *angustifolia*, transpiration is observed to peak at noon, i.e., just before stomatal closure at
93 mid-day under water-deficit conditions (Liu et al., 2011). In contrast, transpiration in
94 *Hedysarum scoparium* peaks multiple times during the day (Xia et al., 2007). Sap flow has
95 been observed to decrease rapidly when the volumetric soil water content (VWC) is lower
96 than the water loss through evapotranspiration (Buzkova et al., 2015). In general, desert
97 shrubs can close their stomata to reduce transpiration when exposed to dehydration stress
98 around mid-day. However, differences exist among shrub species with respect to their
99 stomatal response to changes in soil and air moisture deficits (Pacala et al., 2001). For some
100 shrubs, sap-flow response to precipitation varies from an immediate decline after a heavy
101 rainfall to no observable change after a small rainfall event (Asner et al., 2003; Zheng and
102 Wang, 2014). Sap flow has been found to increase with increasing rainfall intensity (Jian et
103 al., 2016). Drought-insensitive shrubs have relatively strong stomatal regulation and,
104 therefore, tend to be insensitive to soil water deficits and rainfall unlike their drought-
105 sensitive counterparts (Du et al., 2011). In general, understanding the relationship between
106 sap-flow rates in plants and environmental factors is decidedly inconsistent, potentially
107 varying with plant habitat (Liu et al., 2011).

108 *Artemisia ordosica*, a shallow-rooted desert shrub, is the dominant plant species in the
109 Mu Us Desert of northwestern China. The shrubs have an important role in combating
110 desertification and in stabilizing sand dunes (Li et al., 2010). Increases in air temperature and
111 precipitation variability and associated shorter wet periods and longer intervals of periodic

112 drought are expected to ensue with projected climate change (Lioubimtseva and Henebry,
113 2009). During dry periods of the year, sap flow in *Artemisia ordosica* has been observed to
114 be controlled by VWC at about a 30-cm depth in the soil (Li et al., 2014). Sap-flow rate is
115 known to be affected by variation in precipitation patterns. Soil water content, in combination
116 with other environmental factors, may have a significant influence on sap-flow rate (Li et al.,
117 2014; Zheng and Wang, 2014). Thus, understanding the controlling mechanisms of sap flow
118 in desert shrubs as a function of variations in biotic and abiotic factors is greatly needed (Gao
119 et al., 2013; Xu et al., 2007).

120 In this study, we measured stem sap flow in *Artemisia ordosica* and associated
121 environmental variables throughout the growing seasons of 2013-2014 (May-September
122 period of each year) to better understand the environmental controls on the temporal
123 dynamics of sap flow. We believe that our findings will provide further understanding of
124 acclimation processes in desert-shrub species under stress of dehydration.

125

126 **2. Materials and Methods**

127 **2.1 Experimental site**

128 Continuous sap-flow measurements were made at the Yanchi Research Station (37°42'
129 31" N, 107°13' 47" E, 1530 m above mean sea level), Ningxia, northwestern China. The
130 research station is located between the arid and semi-arid climatic zones along the southern
131 edge of the Mu Us Desert. The sandy soil in the upper 10 cm of the soil profile has a bulk
132 density of $1.54 \pm 0.08 \text{ g cm}^{-3}$ (mean \pm standard deviation, n=16). Mean annual precipitation
133 in the region is about 287 mm, of which 62% falls between July and September. Mean annual

134 potential evapotranspiration and air temperature are about 2,024 mm and 8.1°C based on
135 meteorological data (1954-2004) from the Yanchi County weather station. Normally, shrub
136 leaf-expansion, leaf-expanded, and leaf-coloration stages begin in April, June, and
137 September (Chen et al., 2015), respectively.

138

139 **2.2 Environmental measurements**

140 Shortwave radiation (R_s in W m^{-2} ; CMP3, Kipp & Zonen, Netherland), air temperature
141 (T in °C), wind speed (u in m s^{-1} , 034B, Met One Instruments Inc., USA), and relative
142 humidity (RH in %; HMP155A, Väisälä, Finland) were measured simultaneously near the
143 sap-flow measurement plot. Half-hourly data were recorded by data logger (CR3000 data
144 logger, Campbell Scientific Inc., USA). Volumetric soil water content (VWC) at 30-cm
145 depths were measured using three ECH₂O-5TE soil moisture probes (Decagon Devices,
146 USA). In the analysis, we used half-hourly averages of VWC from the three soil moisture
147 probes. Vapor pressure deficit (VPD in kPa) was calculated from recorded RH and T .

148

149 **2.3 Measurements of sap flow, leaf area and stomatal conductance**

150 The experimental plot (10 m × 10 m) was located on the western side of Yanchi Research
151 Station in an *Artemisia ordosica*-dominated area. Mean age of the *Artemisia ordosica* was
152 10-years old. Maximum monthly mean leaf area index (LAI) for plant specimens with full
153 leaf expansion was about 0.1 $\text{m}^2 \text{m}^{-2}$ (Table 1). Over 60% of their roots were distributed in the
154 first 60 cm of the soil complex (Zhao et al., 2010; Jia et al., 2016). Five stems of *Artemisia*
155 *ordosica* were randomly selected within the plot as replicates for sap-flow measurement.

156 Mean height and sapwood area of sampled shrubs were 84 cm and 0.17 cm², respectively.
157 Sampled stems represented the average size of stems in the plot. A heat balance sensor
158 (Flow32-1K, Dynamax Inc., Houston, USA) was installed at about 15 cm above the ground
159 surface on each of the five stems (Dynamax, 2005). Sap-flow measurements from each stem
160 were taken once per minute. Half-hourly data were recorded by a Campbell CR1000 data
161 logger from May 1 to September 30, 2013-2014 (Campbell Scientific, Logan, UT, USA).

162 Leaf area was estimated for each stem every 7-10 days by sampling about 50-70 leaves
163 from five randomly sampled neighboring shrubs with similar characteristics to the shrubs
164 used for sap-flow measurements. Leaf area was measured immediately at the station
165 laboratory with a portable leaf-area meter (LI-3000, Li-Cor, Lincoln, NE, USA). Leaf area
166 index (LAI) was measured at roughly weekly intervals on a 4×4 grid of 16 quadrats (10 m
167 ×10 m each) within a 100 m × 100 m plot centered on the flux tower using measurements of
168 sampled leaves and allometric equations (Jia et al., 2014). Stomatal conductance (g_s) was
169 measured *in situ* for three to four leaves on each of the sampled shrubs with a LI-6400
170 portable photosynthesis analyzer (Li-Cor Inc., Lincoln, USA). The g_s measurements were
171 made every two hours from 7:00 to 19:00 h every ten days from May to September, 2013 and
172 2014.

173 The degree of coupling between the ecosystem surface and the atmospheric boundary
174 layer was estimated with the decoupling coefficient (Ω). The decoupling coefficient varies
175 from 0 (i.e., leaf transpiration is mostly controlled by g_s) to 1 (i.e., leaf transpiration is mostly
176 controlled by radiation). The Ω was calculated as described by Jarvis and McNaughton
177 (1986):

$$178 \quad \Omega = \frac{\Delta + \gamma}{\Delta + \gamma \left(1 + \frac{g_a}{g_s} \right)}, \quad (1)$$

179 where Δ is the rate of change of saturation vapor pressure vs. temperature (kPa K^{-1}), γ is the
 180 psychrometric constant (kPa K^{-1}), and g_a is the aerodynamic conductance (m s^{-1} ; Monteith
 181 and Unsworth, 1990):

$$182 \quad g_a = \left(\frac{u}{u^{*2}} + 6.2u^{*-0.67} \right)^{-1}, \quad (2)$$

183 where u is the wind speed (m s^{-1}) at 6 m above the ground, and u^* is the friction velocity (m
 184 s^{-1}), which was measured using nearby eddy covariance system (Jia et al., 2014).

185

186 **2.4 Data analysis**

187 In our analysis, March-May represented spring, June-August summer, and September-
 188 November autumn (Chen et al., 2015). Drought days were defined as those days with daily
 189 mean VWC $< 0.1 \text{ m}^3 \text{ m}^{-3}$. This is based on a VWC threshold of $0.1 \text{ m}^3 \text{ m}^{-3}$ for J_s (Fig. 1),
 190 with J_s increasing as VWC increased, saturating at VWC of $0.1 \text{ m}^3 \text{ m}^{-3}$, and decreasing as
 191 VWC continued to increase. The VWC threshold of $0.1 \text{ m}^3 \text{ m}^{-3}$ is equivalent to a relative
 192 extractable soil water (REW) of 0.4 for drought conditions (Granier et al., 1999 and 2007;
 193 Zeppel et al., 2004 and 2008; Fig. 2d, e). Duration and severity of ‘drought’ were defined
 194 based on a VWC threshold and REW of 0.4. REW was calculated as from equation (3):

$$195 \quad REW = \frac{VWC - VWC_{\min}}{VWC_{\max} - VWC_{\min}} \quad (3)$$

196 where VWC is the specific daily soil water content ($\text{m}^3 \text{ m}^{-3}$), VWC_{\min} and VWC_{\max} are the
 197 minimum and maximum VWC during the measurement period in each year, respectively.

198 Sap-flow analysis was conducted using mean data from five sensors. Sap flow per leaf
199 area (J_s) was used in this study, i.e.,

$$200 \quad J_s = \left(\sum_{i=1}^n E_i / A_{li} \right) / n \quad (4)$$

201 where, J_s is the sap flow per leaf area ($\text{kg m}^{-2} \text{h}^{-1}$) or ($\text{kg m}^{-2} \text{d}^{-1}$), E is the measured sap flow
202 of a stem (g h^{-1}), A_l is the leaf area of the sap-flow stem, and “ n ” is the number of stems used
203 ($n = 5$).

204 Transpiration per ground area (T_r) was estimated in this study according to:

$$205 \quad T_r = \left(\sum_{i=1}^n J_s \times LAI \right) / n \quad (5)$$

206 where, T_r is transpiration per ground area (mm d^{-1}), and LAI is the leaf area index (m^2
207 m^{-2}).

208 Linear and non-linear regressions were used to analyze abiotic control on sap-flow rate.
209 In order to minimize the effects of different phenophases and rainfall, we used data only from
210 mid-growing season, non-rainy days, and daytime measurements (8:00-20:00), i.e., from
211 June 1 to August 31, with hourly shortwave radiation $> 10 \text{ W m}^{-2}$. Relations between mean
212 sap-flow rates at specific times over a period of 8:00-20:00 and corresponding environmental
213 factors from June 1 to August 31 were derived with linear regression ($p < 0.05$; Fig. 3).
214 Regression slopes were used as indicators of sap-flow sensitivity (degree of response) to the
215 various environmental variables (see e.g., Zha et al., 2013). All statistical analyses were
216 performed with SPSS v. 17.0 for Windows software (SPSS Inc., USA). Significance level
217 was set at 0.05.

218

219 **3. Results**

220 **3.1 Seasonal variations in environmental factors and sap flow**

221 **The range of daily** means (24-hour mean) for R_s , T , VPD, and VWC during the 2013 growing
222 season (May-September) were 31.1-364.9 W m^{-2} , 8.8-24.4°C, 0.05-2.3 kPa, and 0.06-0.17
223 $\text{m}^3 \text{m}^{-3}$ (Fig. 2a, b, c, d), respectively, annual means being 224.8 W m^{-2} , 17.7°C, 1.03 kPa,
224 and 0.08 $\text{m}^3 \text{m}^{-3}$. Corresponding range of daily means for 2014 were 31.0-369.9 W m^{-2} , 7.1-
225 25.8°C, 0.08-2.5 kPa, and 0.06-0.16 $\text{m}^3 \text{m}^{-3}$ (Fig. 2a, b, c, d), respectively, annual means being
226 234.9 W m^{-2} , 17.2°C, 1.05 kPa, and 0.09 $\text{m}^3 \text{m}^{-3}$.

227 Total precipitation and number of rainfall events during the 2013 measurement period
228 (257.2 mm and 46 days) were about 5.6% and 9.8% lower than those during 2014 (272.4 mm
229 and 51 days; Fig. 2d), respectively. In 2013, more irregular rainfall events occurred than in
230 2014, with 45.2% of rainfall falling in July and 8.8% in August.

231 Drought mainly occurred in May, June, and August of 2013 and in May and June of
232 2014 (Fig. 2d, e). Both years had dry springs. Over one-month period of summer drought
233 occurred in 2013.

234 **The range of daily** J_s during the growing season was 0.01-4.36 $\text{kg m}^{-2} \text{d}^{-1}$ in 2013 and
235 0.01-2.91 $\text{kg m}^{-2} \text{d}^{-1}$ in 2014 (Fig. 2f), with annual means of 0.89 $\text{kg m}^{-2} \text{d}^{-1}$ in 2013 and 1.31
236 $\text{kg m}^{-2} \text{d}^{-1}$ in 2014. Mean daily J_s over the growing season of 2013 was 32%, lower than that
237 of 2014. Mean daily T_r were 0.05 mm d^{-1} and 0.07 mm d^{-1} over the growing season of 2013
238 and 2014 (Fig. 2f), respectively, being 34% lower in 2013 than in 2014. The total T_r over the
239 growing season (May 1-September 30) of 2013 and 2014 were 7.3 mm and 10.9 mm,
240 respectively. Seasonal fluctuations in J_s and T_r corresponded with seasonal patterns in VWC
241 (Fig. 2d, f). Daily mean J_s and T_r decreased or remained nearly constant during dry-soil

242 periods (Fig. 2d, f), with the lowest J_s and T_r observed in spring and mid-summer (August)
243 of 2013.

244

245 **3.2 Sap flow response to environmental factors**

246 In summer, J_s increased with increasing VWC (Fig. 2d, f; Fig. 3d). Soil water was shown to
247 modify the response of J_s to environmental factors (Fig. 4). Sap flow increased more rapidly
248 with increases in R_s , T , and VPD under high VWC (i.e., $VWC > 0.1 \text{ m}^3 \text{ m}^{-3}$ in both 2013 and
249 2014) compared with periods with lower VWC (i.e., $VWC < 0.1 \text{ m}^3 \text{ m}^{-3}$ in both 2013 and
250 2014). Sap flow J_s was more sensitive to R_s , T , and VPD under high VWC (Fig. 4), which
251 coincided with a larger regression slope under high VWC conditions.

252 Sensitivity of J_s to environmental variables (in particular, R_s , T , VPD, and VWC) varied
253 depending on time of day (Fig. 5). Regression slopes for the relations of J_s - R_s , J_s - T , and J_s -
254 VPD were greater in the morning before 11:00 h, and lower during mid-day and early
255 afternoon (12:00-16:00 h). In contrast, regression slopes of the relation of J_s -VWC were
256 lower in the morning (Fig. 5), increasing thereafter, peaking at ~13:00 h, and subsequently
257 decreasing in late afternoon. Regression slopes of the response of J_s to R_s , T , and VPD in
258 2014 were greater than those in 2013.

259

260 **3.3 Diurnal changes and hysteresis between sap flow and environmental factors**

261 Diurnal patterns of J_s were similar in both years (Fig. 6), initiating at 7:00 h and increasing
262 thereafter, peaking before noon (12:00 h), and subsequently decreasing thereafter and
263 remaining near zero from 20:00 to 6:00 h. Diurnal changes in g_s were similar to J_s , but
264 peaking about 2 and 1 h earlier than J_s in July and August, respectively (Fig. 6).

265 There were pronounced time lags between J_s and R_s over the two years (Fig. 7), J_s peaked
266 earlier than R_s and, thus, earlier than either VPD or T . These time lags differed seasonally.
267 For example, mean time lag between J_s and R_s was 2 h during July, 5 h during May, and 3 h
268 during June, August, and September of 2013. However, the time lags in 2014 were generally
269 shorter than those observed in 2013 (Table 2).

270 Clockwise hysteresis loops between J_s and R_s during the growing period were observed
271 (Fig. 7). As R_s increased in the morning, J_s increased until it peaked at ~10:00 h. Sap-flow
272 rate declined with decreasing R_s during the afternoon. Sap flow J_s was higher in the morning
273 than in the afternoon, forming a clockwise hysteresis loop.

274 Diurnal time lag in the relation of J_s - R_s were influenced by VWC (Fig. 8, 9). For
275 example, J_s peaked about 2 h earlier than R_s on days with low VWC (Fig. 8a), 1 h earlier than
276 R_s on days with moderate VWC (Fig. 8b), and at the same time as R_s on days with high VWC
277 (Fig. 8c). Lag hours between J_s and R_s over the growing season were negatively and linearly
278 related to VWC (Fig. 9: Lag (h) = $-133.5 \times \text{VWC} + 12.24$, $R^2 = 0.41$). Effect of VWC on time
279 lags between J_s and R_s was smaller in 2014, with evenly distributed rainfall during the
280 growing season, than in 2013, with a pronounced summer drought (Fig. 9). State variables g_s
281 and Ω showed a significantly increasing trend with increasing VWC in 2013 and 2014,
282 respectively (Fig. 10).

283

284 **4. Discussion and conclusions**

285 **4.1 Sap flow response to environmental factors**

286 Drought tolerance of some plants may be related to lower overall sensitivity of plant

287 physiological attributes to environmental stress and/or stomatal regulation (Huang et al.,
288 2011b; Naithani et al., 2012). In this study, large regression slopes between J_s and the
289 environmental variables (R_s , VPD, and T) in the morning indicated that sap flow was more
290 sensitive to variations in R_s , VPD, and T during the drier and hotter period of the day (Fig.
291 5). Stomatal conductances were the largest in the morning (Fig. 6), which led to increases in
292 water fluxes to the atmosphere as a result of increased R_s , T , and VPD. When R_s peaked
293 during mid-day (13:00-14:00 h), there was often insufficient soil water to meet the
294 atmospheric demand for water, causing g_s to be limited by available soil moisture and making
295 J_s more responsive to VWC at noon, but less responsive to R_s and T . Similarly, *Hedysarum*
296 *mongolicum* in a nearby region positively correlated with VWC at noon (Qian et al., 2015),
297 and the evapotranspiration of a Scots pine stand showed higher sensitivity to surface
298 conductance, temperature, vapor pressure deficit, and radiation in the morning than in the
299 afternoon (Zha et al., 2013).

300 Synergistic interactions among environmental factors influencing sap flow are complex.
301 In general, VWC has an influence on physiological processes of plants in water-limited
302 ecosystems (Lei et al., 2010; She et al., 2013). Our finding regarding lower sensitivity in J_s
303 to environmental factors (R_s , T and VPD) during dry periods was consistent with an earlier
304 study of boreal grasslands (Zha et al., 2010). Also our finding that VWC is the most important
305 factor modifying responses in sap flow in *Artemisia ordosica* to other environmental factors,
306 is in contrast to other shrub species. For example, it has been found that sap flow in *Haloxylon*
307 *ammodendron* in northwest China, where annual precipitation is 37.9 mm and mean annual
308 temperature is 8.2 °C, was mainly controlled by T (Zhang et al., 2003), while sap flow in

309 *Cyclobalanopsis glauca* in south China, where annual precipitation is 1900 mm and mean
310 annual temperature is 19.3 °C, was controlled by R_s and T , when VWC was not limiting
311 (Huang et al., 2009).

312 Precipitation, being the main source of VWC at our site, affected transpiration directly.
313 In this sense, frequent small rainfall events (< 5 mm) were important to the survival and
314 growth of the desert plants (Sala and Lauenroth, 1982; Zhao and Liu, 2010). Variations in J_s
315 were clearly associated with the intermittent supply of water to the soil during rainfall events,
316 as revealed at our site (Fig. 2d, f). Reduced J_s during rainy days can be explained by a
317 reduction in incident R_s and water-induced saturation on the leaf surface, which led to a
318 decrease in leaf turgor and stomatal closure. After each rainfall event, J_s increased quickly
319 when soil water was replenished. Schwinning and Sala (2004) showed previously for similar
320 research sites that VWC contributed the most to the response in plant transpiration to post-
321 rainfall events. We showed in this study that *Artemisia ordosica* responded in a different way
322 to wet and dry conditions. In the mid-growing season, high J_s in July were related to rainfall-
323 fed VWC, which increased the rate of transpiration. However, dry soil conditions combined
324 with high T and R_s , led to a reduction in J_s in August of 2013 (Fig. 2). In some desert shrubs,
325 groundwater may replenish water lost by transpiration by having deep roots (Yin et al., 2014).
326 *Artemisia ordosica* roots are generally distributed in the upper 60 cm of the soil (Zhao et al.,
327 2010; Wang et al., 2016), and as a result the plant usually depends on water directly supplied
328 by precipitation because groundwater levels in drylands can be well below the rooting zone,
329 typically, at depths ≥ 10 m at our site.

330

331 4.2 Hysteresis between sap flow and environmental factors

332 Diurnal patterns in J_s corresponded with those of R_s from sunrise until diverging later in the
333 day (Fig. 7), suggesting that R_s was a primary controlling factor of diurnal variation in J_s .
334 According to O'Brien et al. (2004), diurnal variation in R_s could cause change in the diurnal
335 variation in the consumption of water. As an initial energy source, R_s can force T and VPD
336 to increase, causing a phase difference in time lags among the relations J_s - R_s , J_s - T , and J_s -
337 VPD.

338 We found a consistent clockwise hysteresis loop between J_s and R_s over a diurnal cycle
339 (Fig. 7). This hysteresis may be due to stomatal conductance being inherently dependent on
340 plant hydrodynamics (Matheny et al. 2014). The large g_s in the morning promoted higher
341 rates of transpiration (Fig. 6, 7), while lower g_s in the afternoon reduced transpiration.
342 Therefore, diurnal curves (hysteresis) were mainly caused by the g_s -induced hydraulic
343 process (Fig. 7). The finding that hysteresis varied seasonally, decreasing with increasing
344 VWC, further supports the hydrodynamic explanation of hysteresis. At our site, dry soils
345 accompanied with high VPD in summer, led to a decreased in g_s and greater control of the
346 stomata on J_s relative to other environmental factors. The result that g_s increased with
347 increasing VWC (Fig. 10a), along with the synchronization of J_s and g_s , suggests that J_s is
348 more sensitive to g_s in low VWC and less so to R_s . Due to the incidence of small rainfall
349 events in desert drylands, soil water supplied by rainfall pulses was largely insufficient to
350 meet the transpiration demand under high mid-day R_s , resulting in clockwise loops. Lower Ω
351 values (< 0.4) at our site also support the idea that VPD and g_s have a greater control on
352 transpiration than R_s (Fig. 10). Contrary to our findings, counterclockwise hysteresis has been

353 observed to occur between transpiration (J_s) and R_s in tropical and temperate forests (Meinzer
354 et al., 1997; O'Brien et al., 2004; Zeppel et al., 2004), which was reported to be consistent
355 with the capacitance in soil-plant-atmosphere systems; it usually takes time for water to move
356 up and expand vascular elements in tree stem during the transition from night to day.

357

358 **4.3. Conclusions**

359 Drought during the leaf-expansion and leaf-expanded periods led to a greater decline in J_s ,
360 causing J_s to be lower in 2013 than in 2014. The relative influence of R_s , T , and VPD on J_s in
361 *Artemisia ordosica* was modified by volumetric soil water content, indicating J_s 's lessened
362 sensitivity to environmental variables (R_s , T and VPD) during dry periods. Sap flow J_s was
363 constrained by soil water deficiency, causing J_s to peak several hours prior to R_s . Diurnal
364 hysteresis between J_s and R_s varied seasonally and was mainly controlled by hydrodynamic
365 stresses. According to this study, soil moisture controlled sap-flow response in *Artemisia*
366 *ordosica*. This species is capable to tolerate and adapt to soil water deficits and drought
367 conditions during the growing season. Altogether, our findings add to our understanding of
368 acclimation in desert-shrub species under stress of dehydration. The knowledge gain can
369 assist in modeling desert-shrub-ecosystem functioning under changing climatic conditions.

370 **Acknowledgments:** This research was financially supported by grants from the National
371 Natural Science Foundation of China (NSFC No. 31670710, 31670708, 31361130340,
372 31270755), the National Basic Research Program of China (Grant No. 2013CB429901), and
373 the Academy of Finland (Project No. 14921). Xin Jia and Wei Feng are also grateful to
374 financial support from the Fundamental Research Funds for the Central Universities (Proj.

375 No. 2015ZCQ-SB-02). This work is related to the Finnish-Chinese collaborative research
376 project EXTREME (2013-2016), between Beijing Forestry University (team led by Prof.
377 Tianshan Zha) and the University of Eastern Finland (team led by Prof. Heli Peltola), and the
378 U.S. China Carbon Consortium (USCCC). We thank Ben Wang, Sijing Li, Qiang Yang, and
379 others for their assistance in the field.

380

381 **References**

382 Asner, G. P., Archer, S., Hughes, R. F., Ansley, R. J., and Wessman, C. A.: Net changes in regional woody
383 vegetation cover and carbon storage in Texas Drylands, 1937–1999, *Global Change Biol.*, 9, 316-
384 335, 2003.

385 Buzkova, R., Acosta, M., Darenova, E., Pokorny, R., and Pavelka, M.: Environmental factors influencing
386 the relationship between stem CO₂ efflux and sap flow, *Trees-Struct. Funct.*, 29, 333-343, 2015.

387 Chen, Z., Zha, T. S., Jia, X., Wu, Y., Wu, B., Zhang, Y., Guo, J., Qin, S., Chen, G., Peltola, H.: Leaf
388 nitrogen is closely coupled to phenophases in a desert shrub ecosystem in China, *J. Arid Environ.*,
389 120, 33-41, 2015.

390 Du, S., Wang, Y. L., Kume, T., Zhang, J. G., Otsuki, K., Yamanaka, N., and Liu, G. B.: Sapflow
391 characteristics and climatic responses in three forest species in the semiarid Loess Plateau region of
392 China, *Agr. Forest Meteorol.*, 151, 1-10, 2011.

393 Dynamax: Dynagage® Installation and Operation Manual, Dynamax, Houston, TX, 2005.

394 Eberbach, P. L. and Burrows, G. E.: The transpiration response by four topographically distributed
395 Eucalyptus species, to rainfall occurring during drought in south eastern Australia, *Physiol. Plant.*,
396 127, 483-493, 2006.

397 Forner, A., Aranda, I., Granier, A., and Valladares, F.: Differential impact of the most extreme drought

398 event over the last half century on growth and sap flow in two coexisting Mediterranean trees, *Plant*
399 *Ecol.*, 215, 703-719, 2014.

400 Gao, Q., Yu, M., and Zhou, C.: Detecting the Differences in Responses of Stomatal Conductance to
401 Moisture Stresses between Deciduous Shrubs and Artemisia Subshrubs, *Plos One*, 8, e84200, 2013.

402 Granier, A., Bréda, N., Biron, P., and Villette, S.: A lumped water balance model to evaluate duration and
403 intensity of drought constraints in forest stands. *Ecol. Model.*, 116, 269–283, 1999.

404 Granier, A., Reichstein M., Bréda N., Janssens I. A., Falge E., Ciais P., Grünwald T., Aubinet M.,
405 Berbigier P., Bernhofer C., Buchmann N., Facini O., Grassi G., Heinesch B., Ilvesniemi H., Kerone
406 P., Knohl A., Köstner B., Lagergren F., Lindroth A., Longdoz B., Loustau D., Mateus J., Montagnani
407 L., Nys C., Moors E., Papale D., Peiffer M., Pilegaard K., Pita G., Pumpanen J., Rambal S., Rebmann
408 C., Rodrigues A., Seufert G., Tenhunen J., Vesala T., and Wang Q.: Evidence for soil water control
409 on carbon and water dynamics in European forests during the extremely dry year: 2003. *Agr. Forest*
410 *Meteorol.*, 143, 123-145, 2007.

411 Houghton, R. A., Hackler, J. L., and Lawrence, K. T.: The U.S. Carbon Budget: Contributions from Land-
412 Use Change, *Science*, 285, 574-578, 1999.

413 Huang, L., Zhang, Z. S., and Li, X. R.: Sap flow of *Artemisia ordosica* and the influence of environmental
414 factors in a revegetated desert area: Tengger Desert, China. *Hydrol. Process.*, 24, 1248–1253, 2010.

415 Huang, H., Gang, W., and NianLai, C.: Advanced studies on adaptation of desert shrubs to environmental
416 stress, *Sci. Cold Arid Regions*, 3, 0455–0462, 2011a.

417 Huang, Y., Li, X., Zhang, Z., He, C., Zhao, P., You, Y., and Mo, L.: Seasonal changes in *Cyclobalanopsis*
418 *glauca* transpiration and canopy stomatal conductance and their dependence on subterranean water
419 and climatic factors in rocky karst terrain, *J. Hydrol.*, 402, 135-143, 2011b.

420 Huang, Y., Zhao, P., Zhang, Z., Li, X., He, C., and Zhang, R.: Transpiration of *Cyclobalanopsis glauca*
421 (syn. *Quercus glauca*) stand measured by sap-flow method in a karst rocky terrain during dry season,
422 *Ecol. Res.*, 24, 791-801, 2009.

423 Jacobsen, A. L., Agenbag, L., Esler, K. J., Pratt, R. B., Ewers, F. W., and Davis, S. D.: Xylem density,
424 biomechanics and anatomical traits correlate with water stress in 17 evergreen shrub species of the
425 Mediterranean-type climate region of South Africa, *J. Ecol.*, 95, 171-183, 2007.

426 Jarvis, P. G. and McNaughton, K. G.: Stomatal Control of Transpiration: Scaling Up from Leaf to Region.
427 In: *Advances in Ecological Research*, MacFadyen, A. and Ford, E. D. (Eds.), Academic Press, 1986.

428 Jia, X., Zha, T.S., Wu, B., Zhang, Y., Gong, J., Qin, S., Chen, G., Kellomki, S. & Peltola, H.: Biophysical
429 controls on net ecosystem CO₂ exchange over a semiarid shrubland in northwest China.
430 *Biogeosciences*, 11, 4679-4693, 2014.

431 Jia, X., Zha, T. S., Gong, J., Wang, B., Zhang Y., Wu B., Qin S., and Peltola H.: Carbon and water exchange
432 over a temperate semi-arid shrubland during three years of contrasting precipitation and soil
433 moisture patterns. *Agr. Forest Meteorol.*, 228, 120-129, 2016.

434 Jian, S. Q., Wu, Z. N., Hu, C. H., and Zhang, X. L.: Sap flow in response to rainfall pulses for two shrub
435 species in the semiarid Chinese Loess Plateau, *J. Hydrol. Hydromech.*, 64, 121-132, 2016.

436 Lei, H., Zhi-Shan, Z., and Xin-Rong, L.: Sap flow of *Artemisia ordosica* and the influence of
437 environmental factors in a revegetated desert area: Tengger Desert, China, *Hydrol. Process.*, 24,
438 1248-1253, 2010.

439 Li, S., Werger, M. A., Zuidema, P., Yu, F., and Dong, M.: Seedlings of the semi-shrub *Artemisia ordosica*
440 are resistant to moderate wind denudation and sand burial in Mu Us sandland, China, *Trees*, 24, 515-
441 521, 2010.

442 Li, S., Zha, T., Qin, S., Qian, D., and Jia, X.: Temporal patterns and environmental controls of sap flow in
443 *Artemisia ordosica*, *Chinese J. Ecol.*, 33, 1-7, 2014.

444 Lioubimtseva, E. and Henebry, G. M.: Climate and environmental change in arid Central Asia: Impacts,
445 vulnerability, and adaptations, *J. Arid Environ.*, 73, 963-977, 2009.

446 Liu, B., Zhao, W., and Jin, B.: The response of sap flow in desert shrubs to environmental variables in an
447 arid region of China, *Ecohydrology*, 4, 448-457, 2011.

448 Matheny, A. M., Bohrer, G., Stoy, P. C., Baker, I. T., Black, A. T., Desai, A. R., Dietze, M. C., Gough, C.
449 M., Ivanov, V. Y., Jassal, R. S., Novick, K. A., Schäfer, K. V. R., and Verbeeck, H.: Characterizing
450 the diurnal patterns of errors in the prediction of evapotranspiration by several land-surface models:
451 An NACP analysis, *J Geophys. Res.: Biogeosciences*, 119, 1458-1473, 2014.

452 Meinzer, F. C., Andrade, J. L., Goldstein, G., Holbrook, N. M., Cavelier, J., and Jackson, P.: Control of
453 transpiration from the upper canopy of a tropical forest: the role of stomatal, boundary layer and
454 hydraulic architecture components, *Plant Cell Environ.*, 20, 1242-1252, 1997.

455 Monteith, J. L. and Unsworth, M. H.: *Principles of Environmental Physics*. Butterworth-Heinemann:
456 Oxford, 1990.

457 Naithani, K. J., Ewers, B. E., and Pendall, E.: Sap flux-scaled transpiration and stomatal conductance
458 response to soil and atmospheric drought in a semi-arid sagebrush ecosystem, *J. Hydrol.*, 464, 176-
459 185, 2012.

460 O'Brien, J. J., Oberbauer, S. F., and Clark, D. B.: Whole tree xylem sap flow responses to multiple
461 environmental variables in a wet tropical forest, *Plant Cell Environ.*, 27, 551-567, 2004.

462 Pacala, S. W., Hurtt, G. C., Baker, D., Peylin, P., Houghton, R. A., Birdsey, R. A., Heath, L., Sundquist,
463 E. T., Stallard, R. F., Ciais, P., Moorcroft, P., Caspersen, J. P., Shevliakova, E., Moore, B., Kohlmaier,

464 G., Holland, E., Gloor, M., Harmon, M. E., Fan, S.-M., Sarmiento, J. L., Goodale, C. L., Schimel, D.,
465 and Field, C. B.: Consistent Land- and Atmosphere-Based U.S. Carbon Sink Estimates, *Science*, 292,
466 2316-2320, 2001.

467 Qian, D., Zha, T. S., Jia, X., Wu, B., Zhang, Y., Bourque C. P. A., Qin, S., and Peltola, H.: Adaptive,
468 water-conserving strategies in *Hedysarum mongolicum* endemic to a desert shrubland ecosystem,
469 *Environ. Earth. Sci.*, 74, 6039–6046, 2015.

470 Razzaghi, F., Ahmadi, S. H., Adolf, V. I., Jensen, C. R., Jacobsen, S. E., and Andersen, M. N.: Water
471 Relations and Transpiration of Quinoa (*Chenopodium quinoa* Willd.) Under Salinity and Soil Drying,
472 *J. Agron. Crop Sci.*, 197, 348-360, 2011.

473 Sala, O. E., and Lauenroth, W. K.: Small rainfall events: an ecological role in semi-arid regions, *Oecologia*,
474 53 (3), 301-304, 1982.

475 Schwinning, S. and Sala, O. E.: Hierarchy of responses to resource pulses in arid and semi-arid ecosystems,
476 *Oecologia*, 141, 211-220, 2004.

477 She, D., Xia, Y., Shao, M., Peng, S., and Yu, S.: Transpiration and canopy conductance of *Caragana*
478 *korshinskii* trees in response to soil moisture in sand land of China, *Agroforest. Syst.*, 87, 667-678,
479 2013.

480 Vilagrosa, A., Bellot, J., Vallejo, V. R., and Gil - Pelegrín, E.: Cavitation, stomatal conductance, and leaf
481 dieback in seedlings of two co - occurring Mediterranean shrubs during an intense drought, *J. Exp.*
482 *Bot.*, 54, 2015-2024, 2003.

483 Wang, B., Zha, T. S., Jia, X., Gong, J.N., Wu, B., Bourque, C. P. A., Zhang, Y., Qin, S., Chen, G., Peltola,
484 H.: Microtopographic variation in soil respiration and its controlling factors vary with plant
485 phenophases in a desert–shrub ecosystem. *Biogeosciences*, 12, 5705-5714, 2015.

486 Xia, G., Kang, S., Du, T., Yang, X., and Zhang, J.: Transpiration of *Hedysarum scoparium* in arid desert
487 region of Shiyang River basin, Gansu Province, Chinese J. Appl. Ecol., 18, 1194-1202, 2007.

488 Xia, G., Kang, S., Li, F., Zhang, J., and Zhou, Q.: Diurnal and seasonal variations of sap flow of *Caragana*
489 *korshinskii* in the arid desert region of north-west China, Hydrol. Process., 22, 1197-1205, 2008.

490 Xu, D. H., Li, J. H., Fang, X. W., and Wang, G.: Changes in soil water content in the rhizosphere of
491 *Artemisia ordosica*: Evidence for hydraulic lift, J. Arid Environ., 69, 545-553, 2007.

492 Yang, Y. and Zhu, Y.: Plant Ecology (Second Edition), Higher Education Press, Beijing, 2011.

493 Yin, L., Zhou, Y., Huang, J., Wenninger, J., Hou, G., Zhang, E., Wang, X., Dong, J., Zhang, J., and
494 Uhlenbrook, S.: Dynamics of willow tree (*Salix matsudana*) water use and its response to
495 environmental factors in the semi-arid Hailiutu River catchment, Northwest China, Environ. Earth
496 Sci., 71, 4997-5006, 2014.

497 Yu, M., Ellis, J. E., and Epstein, H. E.: Regional analysis of climate, primary production, and livestock
498 density in Inner Mongolia. J. Environ. Qual., 33(5), 1675-1681, 2004.

499 Zeppel, M. J. B., Murray, B. R., Barton, C., and Eamus, D.: Seasonal responses of xylem sap velocity to
500 VPD and solar radiation during drought in a stand of native trees in temperate Australia, Funct. Plant
501 Biol., 31, 461-470, 2004.

502 Zeppel, M. J. B., Macinnis-Ng, C. M. O., Yunusa, I. A. M., Whitley, R. J., and Eamus, D. Long term
503 trends of stand transpiration in a remnant forest during wet and dry years, J. Hydrol., 349, 200-213,
504 2008.

505 Zha, T. S., Barr, A. G., Kamp, G. V. D., Black, T.A., McCaughey, J. H., and Flanagan, L.B.: Interannual
506 variation of evapotranspiration from forest and grassland ecosystems in western Canada in relation
507 to drought, Agr. Forest Meteorol., 150, 1476-1484, 2010.

508 Zha, T. S., Li, C., Kellomäki, S., Peltola, H., Wang, K.-Y., and Zhang, Y.: Controls of Evapotranspiration
509 and CO₂ Fluxes from Scots Pine by Surface Conductance and Abiotic Factors, *Plos One*, 8, e69027,
510 2013.

511 Zhang, X., Gong, J., Zhou, M., and Si, J.: A study on the stem sap flow of *Populus euphratica* and *Tamaris*
512 spp. By heat pulse technique, *J. Glaciol. Geocryol.*, 25, 584-590, 2003.

513 Zhao, W. and Liu, B.: The response of sap flow in shrubs to rainfall pulses in the desert region of China,
514 *Agr. Forest Meteorol.*, 150, 1297-1306, 2010.

515 Zhao, Y., Yuan, W., Sun, B., Yang, Y., Li, J., Li, J., Cao, B., and Zhong, H.: Root Distribution of Three
516 Desert Shrubs and Soil Moisture in Mu Us Sand Land. *Res. Soil Water Conserv.*, 17, 129-133, 2010.

517 Zhao, W., Liu, B., Chang, X., Yang, Q., Yang, Y., Liu Z., Cleverly, J., and Eamus, D.: Evapotranspiration
518 partitioning, stomatal conductance, and components of the water balance: A special case of a desert
519 ecosystem in China. *J. Hydrol.*, 538, 374-386, 2016.

520 Zheng, C. and Wang, Q.: Water-use response to climate factors at whole tree and branch scale for a
521 dominant desert species in central Asia: *Haloxylon ammodendron*, *Ecohydrology*, 7, 56-63, 2014.

522 Zheng, H., Wang, Q., Zhu, X., Li, Y., and Yu, G.: Hysteresis Responses of Evapotranspiration to
523 Meteorological Factors at a Diel Timescale: Patterns and Causes, *Plos One*, 9, e98857, 2014.

524

525

526

527 **Table 1** Seasonal changes in monthly transpiration (T_r), leaf area index (LAI), and stomatal
 528 conductance (g_s) of *Artemisia ordosica* from 2013 to 2014.
 529

	T_r (mm mon ⁻¹)		LAI (m ² m ⁻²)		g_s (mol m ⁻² s ⁻¹)	
	2013	2014	2013	2014	2013	2014
May	0.57	1.59	0.02	0.04	0.07	0.18
June	1.03	2.28	0.05	0.06	0.08	0.13
July	3.36	3.46	0.10	0.06	0.09	0.14
August	1.04	2.45	0.08	0.06	0.10	0.08
September	1.23	1.13	0.05	0.04	0.15	0.05

530
 531

532 **Table 2** Mean monthly diurnal cycles of sap-flow rate (J_s) response to shortwave radiation
 533 (R_s), air temperature (T), and vapor pressure deficit (VPD), including time lags (h) in J_s as a
 534 function of R_s , T , and VPD.

535

Pattern	May		June		July		August		September	
	2013	2014	2013	2014	2013	2014	2013	2014	2013	2014
J_s - R_s	5	2	3	0	2	1	3	1	3	2
J_s - T	8	6	7	4	4	4	6	5	6	6
J_s -VPD	8	5	7	4	6	4	6	5	6	5

536

537

538

539 **Figure captions:**

540 **Fig. 1** Sap-flow rate per leaf area (J_s) as a function of soil water content (VWC) at 30 cm
541 depth in non-rainy, daytime hours during the mid-growing period from June 1-August 31
542 over 2013-2014. Data points are binned values from pooled data over two years at a VWC
543 increment of $0.003 \text{ m}^3 \text{ m}^{-3}$. Dotted line represents the VWC threshold for J_s .

544 **Fig. 2** Seasonal changes in daily (24-hour) mean shortwave radiation (R_s ; a), air temperature
545 (T ; b), vapor pressure deficit (VPD; c), volumetric soil water content (VWC; d), relative
546 extractable water (REW; e), daily total precipitation (PPT; d), and daily sap-flow per leaf
547 area (J_s ; f), and daily transpiration (T_r , mm d^{-1} ; f) from May to September for both 2013 and
548 2014. Horizontal dash lines (d, e) represent VWC and REW threshold of $0.1 \text{ m}^3 \text{ m}^{-3}$ and 0.4 ,
549 respectively. Shaded bands indicate periods of drought.

550 **Fig. 3** Relationships between sap-flow rate per leaf area (J_s) and environmental factors
551 [shortwave radiation (R_s), air temperature (T), vapor pressure deficit (VPD), and soil water
552 content at 30-cm depth (VWC)] in non-rainy days between 8:00-20:00 h during the mid-
553 growing season of June 1-August 31 for 2013 and 2014. Data points are binned values from
554 pooled data over two years at increments of 40 W m^{-2} , $1.2 \text{ }^\circ\text{C}$, 0.3 kPa , and $0.005 \text{ m}^3 \text{ m}^{-3}$ for
555 R_s , T , VPD and VWC, respectively.

556 **Fig. 4** Sap-flow rate per leaf area (J_s) in non-rainy, daytime hours during the mid-growing
557 season of June 1-August 31 for both 2013 and 2014 as a function of shortwave radiation (R_s),
558 air temperature (T), vapor pressure deficit (VPD) under high volumetric soil water content
559 ($\text{VWC} > 0.10 \text{ m}^3 \text{ m}^{-3}$ both in 2013 and 2014) and low VWC ($< 0.10 \text{ m}^3 \text{ m}^{-3}$, 2013 and 2014).
560 J_s is given as binned averages according to R_s , T , and VPD, based on increments of 100 W

561 m^{-2} , 1°C , and 0.2 kPa , respectively. Bars indicate standard error.

562 **Fig. 5** Regression slopes of linear fits between sap-flow rate per leaf area (J_s) in non-rainy
563 days and shortwave radiation (R_s), vapor pressure deficit (VPD), air temperature (T), and
564 volumetric soil water content (VWC) between 8:00-20:00 h during the mid-growing season
565 of June 1-August 31 for 2013 and 2014.

566 **Fig. 6** Mean monthly diurnal changes in sap-flow rate per leaf area (J_s) and stomatal
567 conductance (g_s) in *Artemisia ordosica* during the growing season (May-September) for both
568 2013 and 2014. Each point is given as the mean at specific times during each month.

569 **Fig. 7** Seasonal variation in hysteresis loops between sap-flow rate per leaf area (J_s) and
570 shortwave radiation (R_s) using normalized plots for both 2013 and 2014. The y-axis
571 represents the proportion of maximum J_s (dimensionless), and the x-axis represents the
572 proportion of maximum R_s (dimensionless). The curved arrows indicate the clockwise
573 direction of response during the day.

574 **Fig. 8** Sap-flow rate per leaf area (J_s) and shortwave radiation (R_s) over consecutive three
575 days in 2013, i.e., (a) under low volumetric soil water content (VWC) and high vapor pressure
576 deficit (VPD; DOY 153-155, $\text{VWC}=0.064 \text{ m}^3 \text{ m}^{-3}$, $\text{REW}=0.025$, $\text{VPD}=2.11 \text{ kPa}$), (b)
577 moderate VWC and VPD (DOY 212-214, $\text{VWC}=0.092 \text{ m}^3 \text{ m}^{-3}$, $\text{REW}=0.292$, $\text{VPD}=1.72$
578 kPa), and (c) high VWC and low VPD (DOY 192-194, $\text{VWC}=0.152 \text{ m}^3 \text{ m}^{-3}$, $\text{REW}=0.865$,
579 $\text{VPD}= 0.46 \text{ kPa}$). REW is the relative extractable soil water. VWC, REW, and VPD are the
580 mean value of the three days.

581 **Fig. 9** Time lag between sap-flow rate per leaf area (J_s) and short wave radiation (R_s) in
582 relation to volumetric soil water content (VWC). Hourly data in non-rainy days during the

583 mid-growing season of June 1-August 31 for 2013 and 2014. The lag hours were calculated

584 by a cross-correlation analysis using a three-day moving window with a one-day time step.

585 Rainy days were excluded. The solid line is based on exponential regression ($p < 0.05$).

586 **Fig. 10** Relationship between volumetric soil water content (VWC) and (a) stomatal

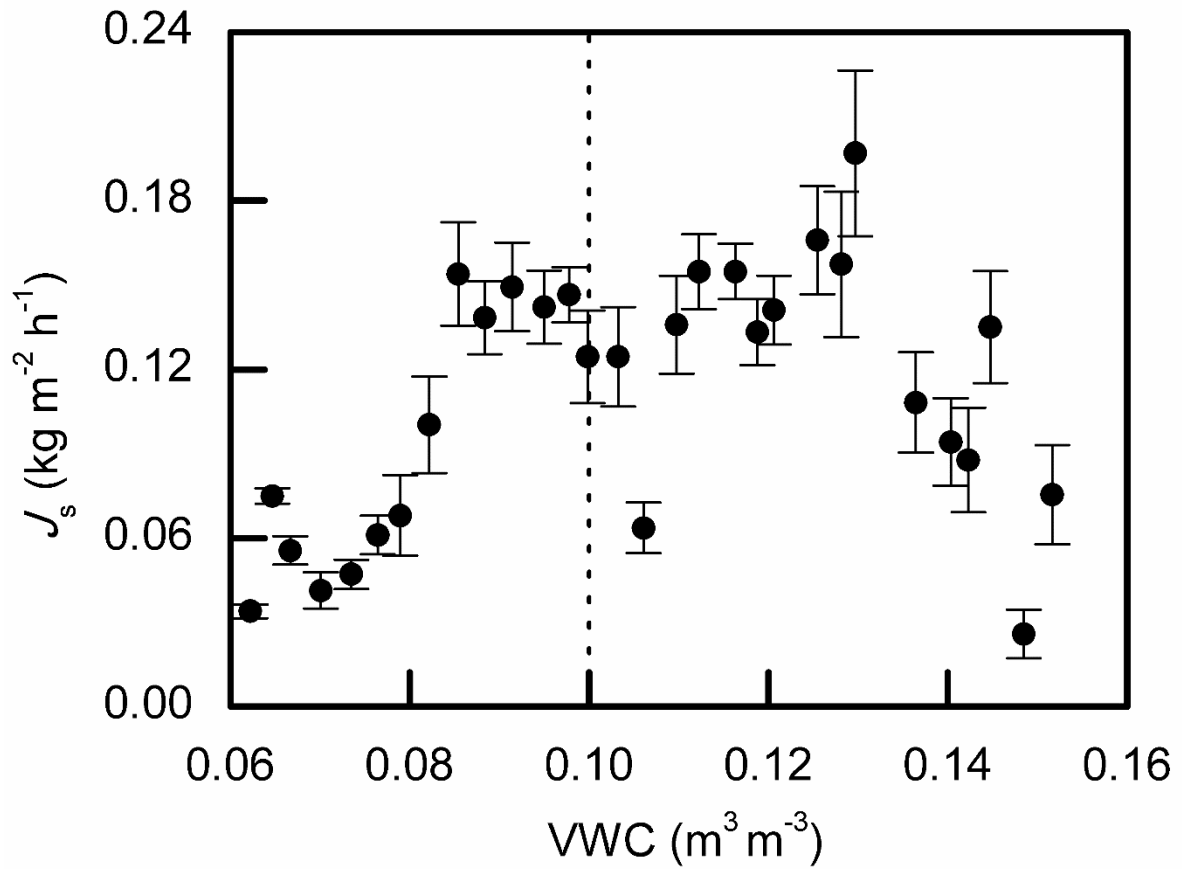
587 conductance (g_s) in *Artemisia ordosica*, and (b) decoupling coefficient (Ω) for 2013 and 2014.

588 Hourly values are given as binned averages based on a VWC-increment of $0.005 \text{ m}^3 \text{ m}^{-3}$.

589 Bars indicate standard error. Only regressions with p -values < 0.05 are shown.

590

591

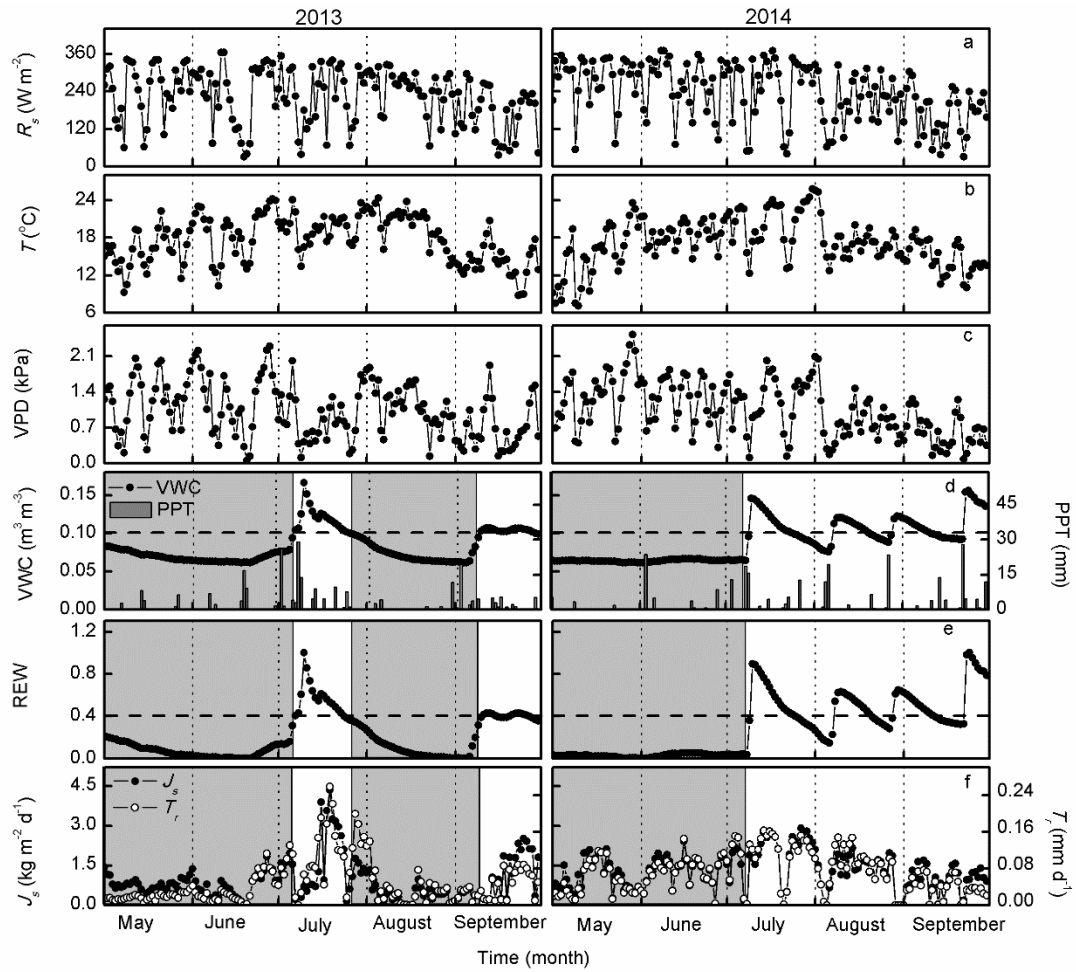


592

593 **Fig. 1** Sap-flow rate per leaf area (J_s) as a function of soil water content (VWC) at 30 cm
594 depth in non-rainy, daytime hours during the mid-growing period from June 1-August 31
595 over 2013-2014. Data points are binned values from pooled data over two years at a VWC
596 increment of $0.003 \text{ m}^3 \text{m}^{-3}$. Dotted line represents the VWC threshold for J_s .

597

598

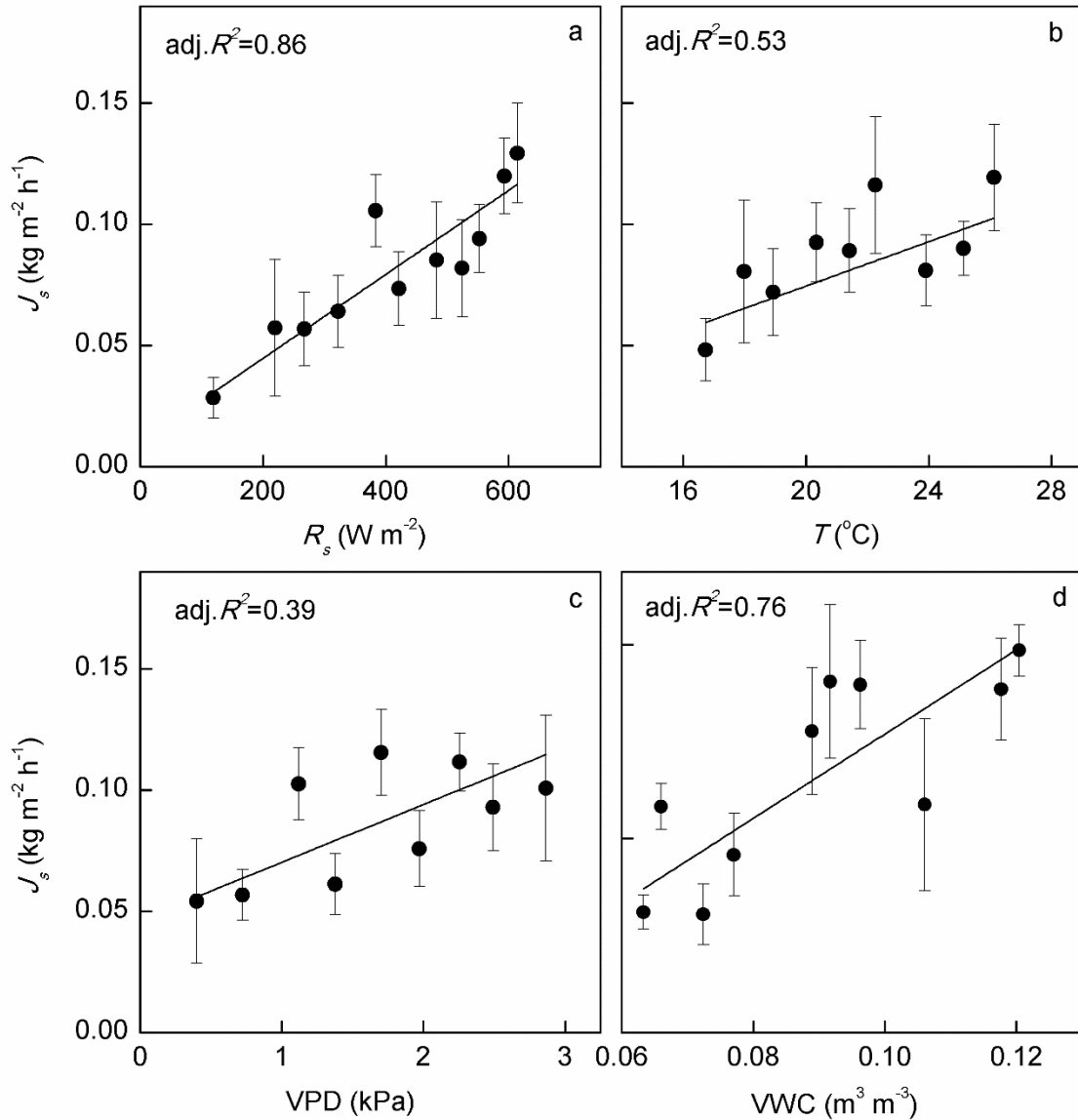


600

601

602 **Fig. 2** Seasonal changes in daily (24-hour) mean shortwave radiation (R_s ; a), air temperature
 603 (T ; b), vapor pressure deficit (VPD; c), volumetric soil water content (VWC; d), relative
 604 extractable water (REW; e), daily total precipitation (PPT; d), and daily sap-flow per leaf
 605 area (J_s ; f), and daily transpiration (T_r , mm d^{-1} ; f) from May to September for both 2013 and
 606 2014. Horizontal dash lines (d, e) represent VWC and REW threshold of $0.1 \text{ m}^3 \text{ m}^{-3}$ and 0.4 ,
 607 respectively. Shaded bands indicate periods of drought.

608



609

610

611 **Fig. 3** Relationships between sap-flow rate per leaf area (J_s) and environmental factors

612 [shortwave radiation (R_s), air temperature (T), vapor pressure deficit (VPD), and soil water

613 content at 30-cm depth (VWC)] in non-rainy days between 8:00-20:00 h during the mid-

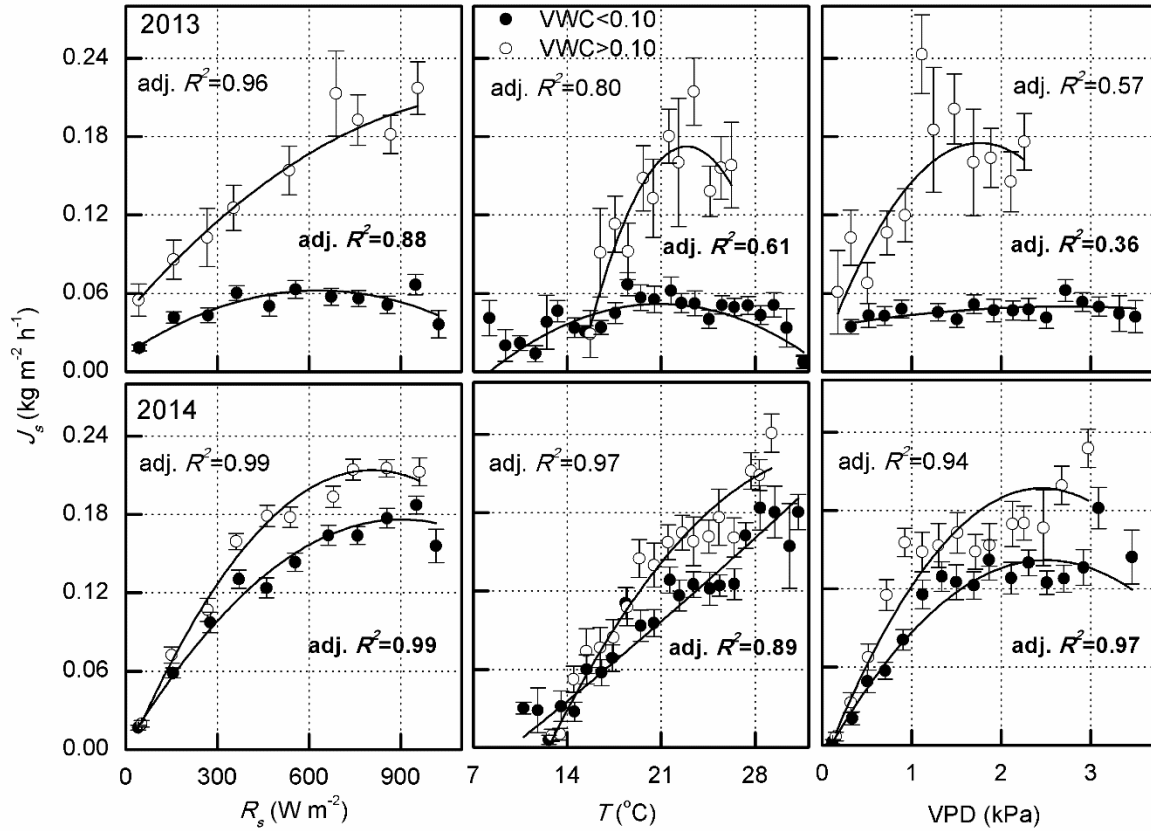
614 growing season of June 1-August 31 for 2013 and 2014. Data points are binned values from

615 pooled data over two years at increments of 40 W m^{-2} , $1.2 \text{ }^{\circ}\text{C}$, 0.3 kPa , and $0.005 \text{ m}^3 \text{ m}^{-3}$ for

616 R_s , T , VPD and VWC, respectively.

617

618



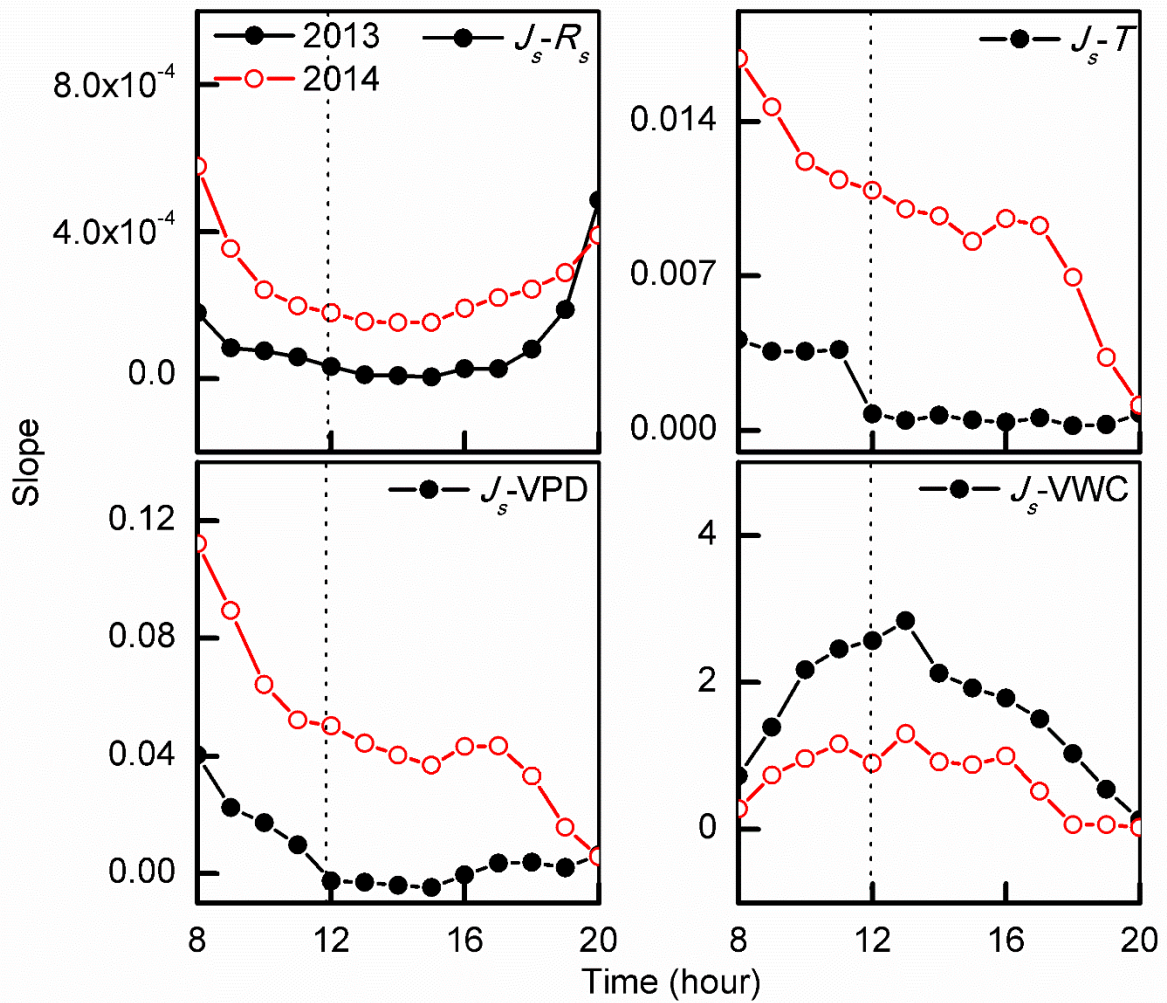
619

620

621 **Fig. 4** Sap-flow rate per leaf area (J_s) in non-rainy, daytime hours during the mid-growing
 622 season of June 1-August 31 for both 2013 and 2014 as a function of shortwave radiation (R_s),
 623 air temperature (T), vapor pressure deficit (VPD) under high volumetric soil water content
 624 ($\text{VWC} > 0.10 \text{ m}^3 \text{ m}^{-3}$ both in 2013 and 2014) and low VWC ($< 0.10 \text{ m}^3 \text{ m}^{-3}$, 2013 and 2014).

625 J_s is given as binned averages according to R_s , T , and VPD, based on increments of 100 W
 626 m^{-2} , 1°C , and 0.2 kPa, respectively. Bars indicate standard error.

627



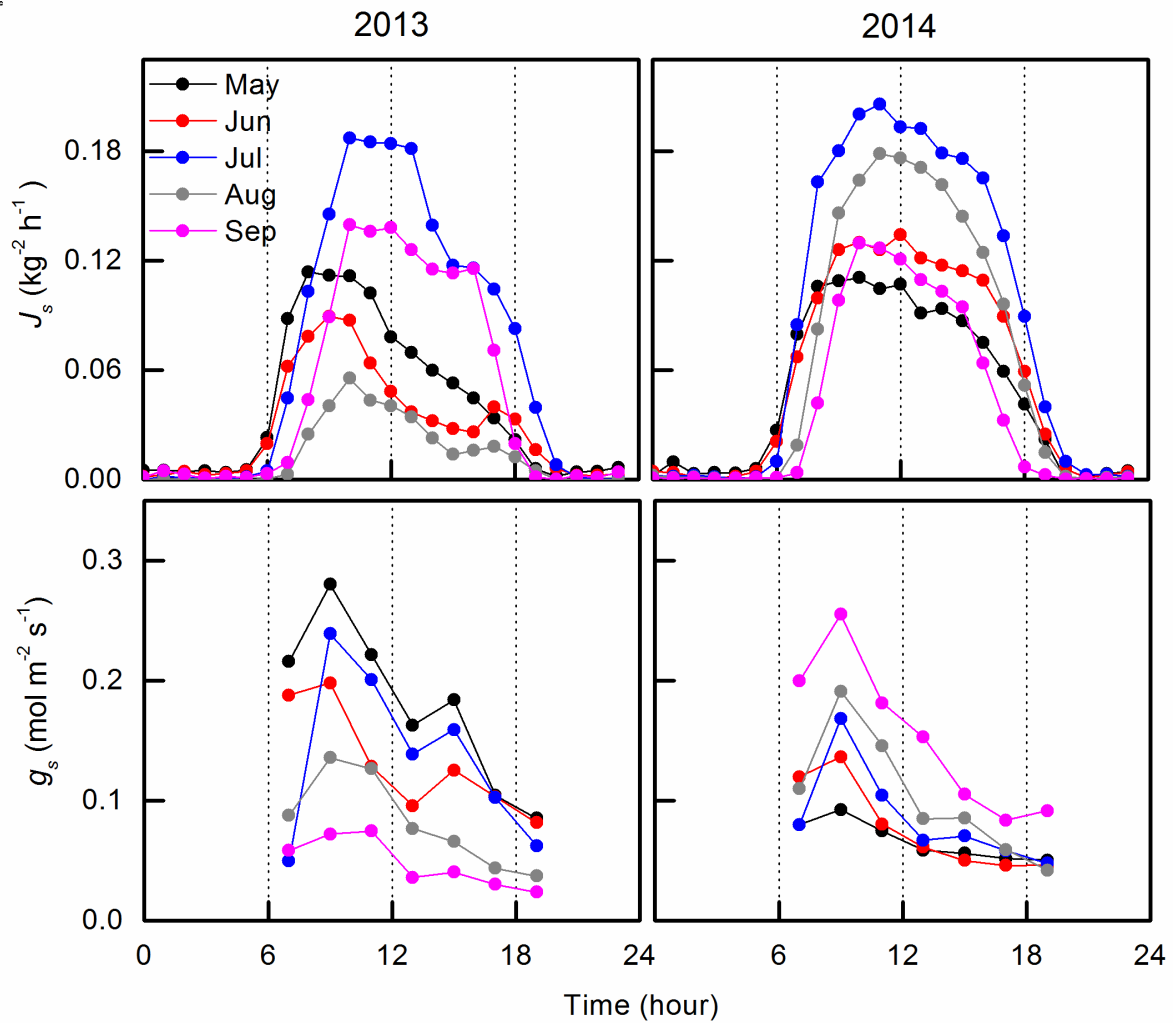
629

630 **Fig. 5** Regression slopes of linear fits between sap-flow rate per leaf area (J_s) in non-rainy631 days and shortwave radiation (R_s), vapor pressure deficit (VPD), air temperature (T), and

632 volumetric soil water content (VWC) between 8:00-20:00 h during the mid-growing season

633 of June 1-August 31 for 2013 and 2014.

634



636

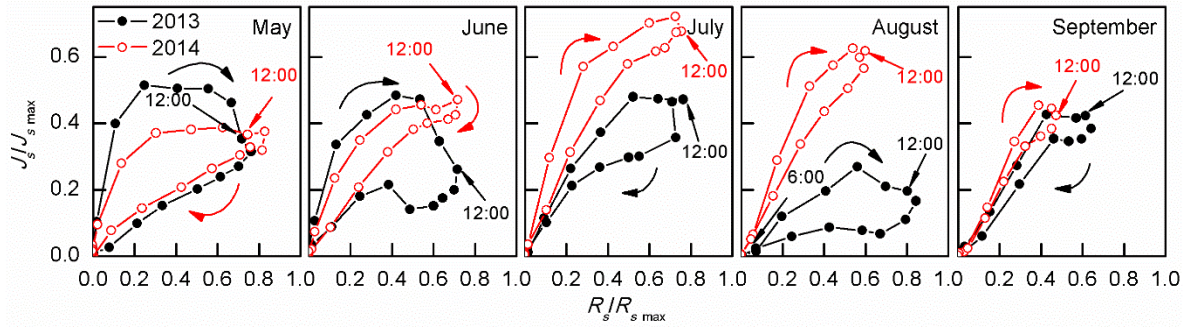
637

638 **Fig. 6** Mean monthly diurnal changes in sap-flow rate per leaf area (J_s) and stomatal
 639 conductance (g_s) in *Artemisia ordosica* during the growing season (May-September) for both
 640 2013 and 2014. Each point is given as the mean at specific times during each month.

641

642

643



644

645

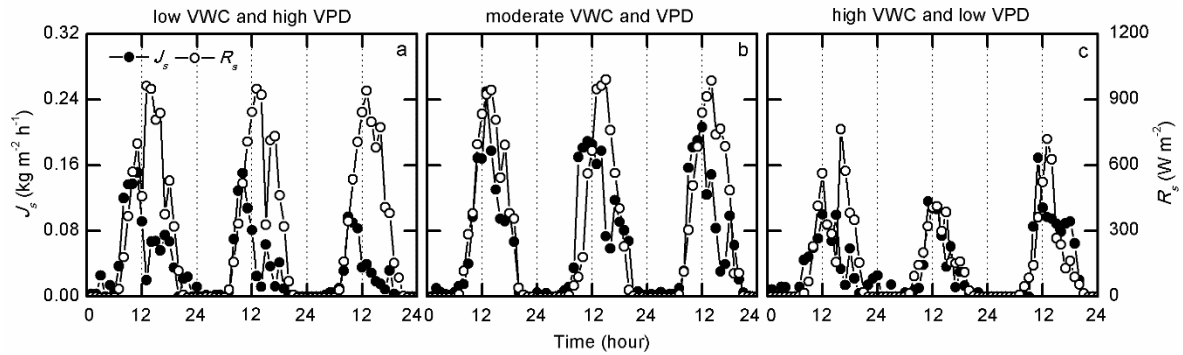
646 **Fig. 7** Seasonal variation in hysteresis loops between sap-flow rate per leaf area (J_s) and
647 shortwave radiation (R_s) using normalized plots for both 2013 and 2014. The y-axis
648 represents the proportion of maximum J_s (dimensionless), and the x-axis represents the
649 proportion of maximum R_s (dimensionless). The curved arrows indicate the clockwise
650 direction of response during the day.

651

652

653

654

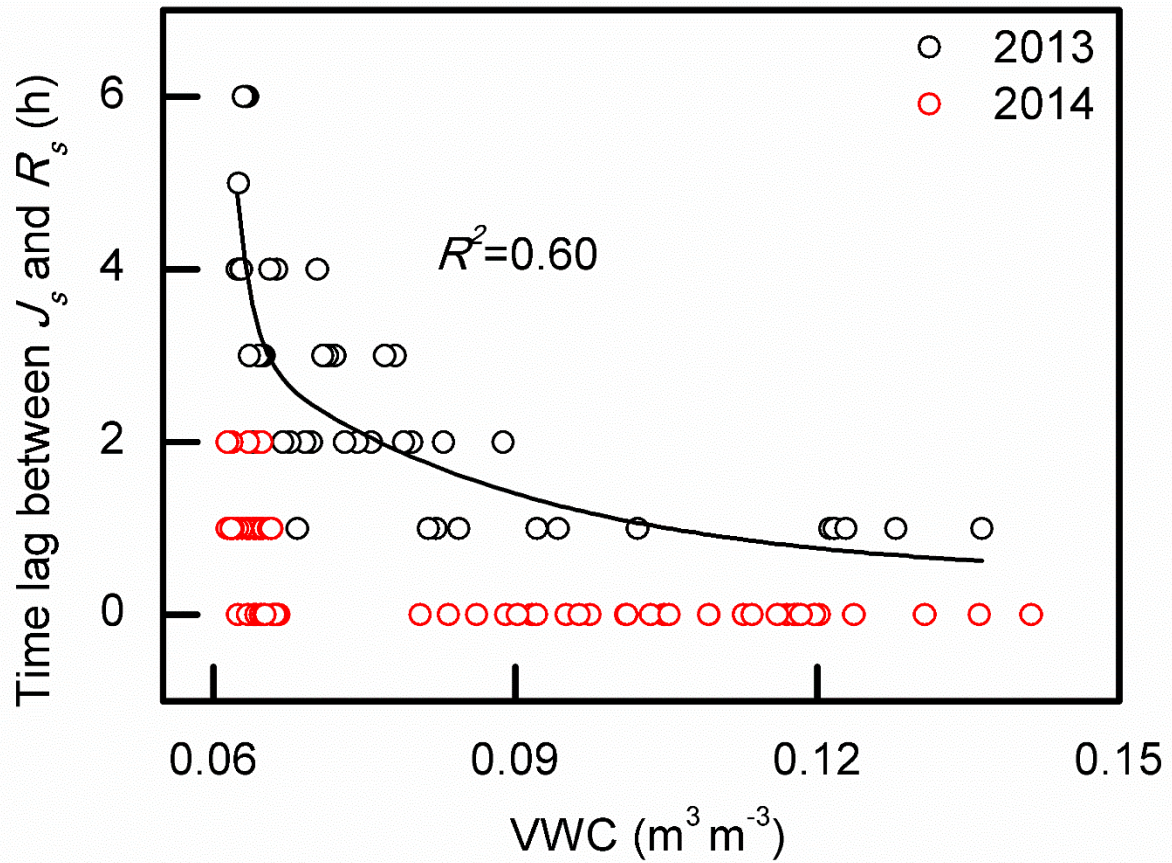


655

656

657 **Fig. 8** Sap-flow rate per leaf area (J_s) and shortwave radiation (R_s) over consecutive three
658 days in 2013, i.e., (a) under low volumetric soil water content (VWC) and high vapor pressure
659 deficit (VPD; DOY 153-155, VWC=0.064 $\text{m}^3 \text{m}^{-3}$, REW=0.025, VPD=2.11 kPa), (b)
660 moderate VWC and VPD (DOY 212-214, VWC=0.092 $\text{m}^3 \text{m}^{-3}$, REW=0.292, VPD=1.72
661 kPa), and (c) high VWC and low VPD (DOY 192-194, VWC=0.152 $\text{m}^3 \text{m}^{-3}$, REW=0.865,
662 VPD= 0.46 kPa). REW is the relative extractable soil water. VWC, REW, and VPD are the
663 mean value of the three days.

664



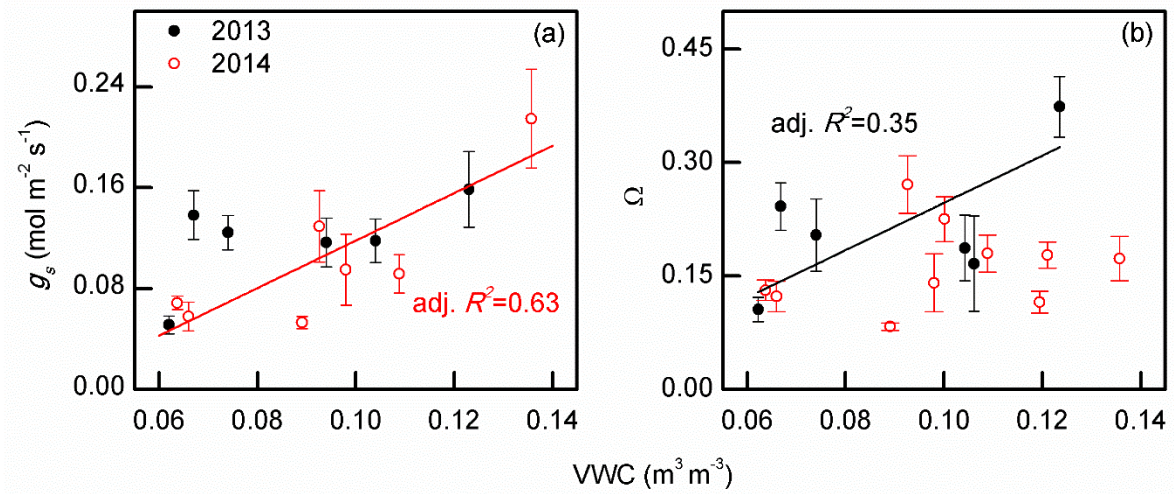
665

666

667 **Fig. 9** Time lag between sap-flow rate per leaf area (J_s) and short wave radiation (R_s) in
 668 relation to volumetric soil water content (VWC). Hourly data in non-rainy days during the
 669 mid-growing season of June 1-August 31 for 2013 and 2014. The lag hours were calculated
 670 by a cross-correlation analysis using a three-day moving window with a one-day time step.
 671 Rainy days were excluded. The solid line is based on exponential regression ($p < 0.05$).

672

673



674

675

676 **Fig. 10** Relationship between volumetric soil water content (VWC) and (a) stomatal
677 conductance (g_s) in *Artemisia ordosica*, and (b) decoupling coefficient (Ω) for 2013 and 2014.

678 Hourly values are given as binned averages based on a VWC-increment of 0.005 m³ m⁻³.

679 Bars indicate standard error. Only regressions with p -values < 0.05 are shown.

680